Falcke, Martin and Moein, Mahsa and Tilunaite, Agne and Thul, Ruediger and Skupin, Alexander (2018) On the phase space structure of IP3 induced Ca2+ signalling and concepts for predictive modeling. Chaos . ISSN 1054-1500 (In Press)

On the phase space structure of IP_3 induced Ca^{2+} signalling and concepts for predictive modeling

Martin Falcke,[1, a)] Mahsa Moein,[2, b)] Agne Tilūnaitė,[3, c)] Rüdiger Thul,[4, d)] and Alexander Skupin[2, 5, e)]

[1)] *Max Delbrück Centre for Molecular Medicine, Robert Rössler Strasse 10, 13125 Berlin, and Dept. of Physics, Humboldt University, Newtonstr. 15, 12489 Berlin, Germany*

[2)] *Luxembourg Centre for Systems Biomedicine, University of Luxembourg, 7, Rue de Swing, Belval, L-4367, Luxembourg*

[3)] *Systems Biology Laboratory, University of Melbourne, Parkville, VIC 3010, Australia*

[4)] *Centre for Mathematical Medicine and Biology, School of Mathematical Sciences, University of Nottingham, NG7 2RD, UK*

[5)] *National Biomedical Computation Resource, University California San Diego, 9500 Gilman Drive, La Jolla, Ca 93121, USA*

(Dated: 10 March 2018)

The correspondence between mathematical structures and experimental systems is the basis of the generalizability of results found with specific systems, and is the basis of the predictive power of theoretical physics. While physicists have confidence in this correspondence, it is less recognized in cellular biophysics. On the one hand, the complex organization of cellular dynamics involving a plethora of interacting molecules and the basic observation of cell variability seem to question its possibility. The practical difficulties of deriving the equations describing cellular behaviour from first principles support these doubts. On the other hand, ignoring such a correspondence would severely limit the possibility of predictive quantitative theory in biophysics. Additionally, the existence of functional modules (like pathways) across cell types suggests also the existence of mathematical structures with comparable universality. Only a few cellular systems have been sufficiently investigated in a variety of cell types to follow up these basic questions. IP_3 induced Ca^{2+} signalling is one of them, and the mathematical structure corresponding to it is subject of ongoing discussion. We review the system's general properties observed in a variety of cell types. They are captured by a reaction diffusion system. We discuss the phase space structure of its local dynamics. The spiking regime corresponds to noisy excitability. Models focussing on different aspects can be derived starting from this phase space structure. We discuss how the initial assumptions on the set of stochastic variables and phase space structure shape the predictions of parameter dependencies of the mathematical models resulting from the derivation.

IP_3 induced Ca^{2+} signalling is one of the most versatile and universal cellular signalling systems and a popular model system in non-linear dynamics for pattern formation in noisy systems. We discuss the experimental evidence allowing for identification of the mathematical structure to which it corresponds, and a variety of concepts for deriving simplified models from it.

I. INTRODUCTION

In spring 1995, I (MF) joined John (Jack) L. Hudson's lab in Charlottesville, Virginia, to work with him on dynamic clustering of globally coupled non-linear oscillators or a topic from pattern formation far from thermodynamic equilibrium. James D. Lechleiter and Patricia Camacho were in Charlottesville at this time, too. James had just published his results on the effect of energizing mitochondria on Ca^{2+} waves in Xenopus oocytes[1], which had several aspects very interesting for the theory of pattern formation. According to that theory, free ends of waves in excitable systems should either form a spiral or recede. The free ends of Ca^{2+} waves with energized mitochondria neither formed spirals nor receded but showed different dynamics. Jack suggested to work on these patterns. This was my first biophysical project and it redirected my career. Jack worked experimentally and developed also the mathematical models explaining his experiments. His high standards and expectations towards theory close to experiments substantially influenced all of my later scientific and educational work.

The first years of this biophysical research led to results on spiral instabilities, spiral pattern regimes and generation and annihilation dynamics[2], but could not explain Lechleiter's experiments. The underlying mathematical structure of the model did not correspond to the experimental system. When we replaced the model with a direct transition from excitability to an oscillatory regime by a model with a direct transition from excitability to bistability[3], it explained not only the mitochondria experiments[4], but also experiments which were not taken into account when it was developed[5]. This exemplifies

---

[a)]Electronic mail: martin.falcke@mdc-berlin.de
[b)]Electronic mail: mahsa.moein@uni.lu
[c)]Electronic mail: agne.tilunaite@unimelb.edu.au
[d)]Electronic mail: ruediger.thul@nottingham.ac.uk
[e)]Electronic mail: alexander.skupin@uni.lu

how the basic mathematical structure of a non-linear dynamical system defined by its set of bifurcations and their relation, often called the bifurcation diagram and phase space structure, is essential for the predictive power of a theoretical description.

In physics, the fundamental equations, like Newton's first law, the variational principles of classical mechanics or the Schrödinger equation of quantum mechanics have been developed with simple examples. Nonetheless, they are stunningly predictive far beyond the systems used in their formulation. This predictive power originates from a correspondence between the experimental objects and mathematical structures. The mechanics of macroscopic objects corresponds to variational principles and differential equations, the behaviour of microscopic objects corresponds to operator theory in Hilbert spaces. The identification of the correct mathematical structure corresponding to an observation provides predictive power to a mathematical theory in science. Mathematical models formulated within mathematical structures not corresponding to the observations still may reproduce the measurements used for their development but rarely are predictive beyond them as illustrated by the history of atom models.

In general, the biophysics of cells has to obey the basic laws of physics - the first principles. But cells consist of many components and interactions and therefore specifying the fundamental equations of physics to a living cell is close to impracticable. The approach of theoretical biophysics is consequently to consider the components and interactions assumed to be most relevant for a specific process of interest and to verify the assumptions retrospectively by contrasting model predictions with experimental results. But does the lack of models derived from first principles for cellular behavior also mean that the correspondence of mathematical structures to observations has no meaning in cellular biophysics? The predictive power growing out of it makes it worth to follow up on this only seemingly philosophical question.

Only a few cellular dynamical systems are currently characterized well enough for identifying the mathematical structure corresponding to them. Intracellular Ca^{2+} dynamics is one of them. The Ca^{2+} pathway translates extracellular signals into intracellular responses by increasing the cytosolic Ca^{2+} concentration in a stimulus dependent pattern[6–8]. The concentration increase can be caused either by Ca^{2+} entry from the extracellular medium through plasma membrane channels, or by Ca^{2+} release from internal storage compartments. In the following, we will focus on inositol 1,4,5-trisphosphate (IP_3)-induced Ca^{2+} release from the endoplasmic reticulum (ER), which is the predominant Ca^{2+} release mechanism in many cell types. IP_3 sensitizes Ca^{2+} channels (IP_3Rs) on the ER membrane for Ca^{2+} binding, such that Ca^{2+} released from the ER through one channel increases the open probability of neighboring channels. This positive feedback of Ca^{2+} on its own release channel is called Ca^{2+}-induced-Ca^{2+}-release (CICR). Open-

ing of an IP_3R triggers a Ca^{2+} flux into the cytosol due to the large concentration differences between the two compartments, which is in the range of 3 to 4 orders of magnitudes. The released Ca^{2+} is removed from the cytosol either by sarco-endoplasmic reticulum Ca^{2+} AT-Pases (SERCAs) into the ER or by plasma membrane Ca^{2+} ATPases into the extracellular space.

IP_3R are spatially organized into clusters of up to about fifteen channels. These clusters are scattered across the ER membrane with distances of 1 to 7 μm[9–13]. CICR and Ca^{2+} diffusion couple the state dynamics of the channels. Given that the diffusion length of free Ca^{2+} is less than 2 μm due to the presence of Ca^{2+} binding molecules in the cytoplasm and SERCAs, the coupling between channels in a cluster is much stronger than the coupling between adjacent clusters[14]. The structural hierarchy of IP_3R from the single channel to clusters shown in Fig. 1 is also reflected in the dynamic responses of the intracellular Ca^{2+} concentration as revealed through fluorescence microscopy and simulations[9,15–17]. Openings of single IP_3R (blips) may trigger collective openings of IP_3R within a cluster (puffs), while Ca^{2+} diffusing from a puff site can then activate neighboring clusters, eventually leading to a global, i.e., cell wide, Ca^{2+} spike[13,16,18,19]. Repetitive sequences of these Ca^{2+} spikes encode information that is used to regulate many processes in various cell types[6,20,21].

Ca^{2+} exerts also a negative feedback on the channel open probability, which acts on a slower time scale than the positive feedback, and has a higher half maximum value than CICR[9,15,18,22–24]. This Ca^{2+}-dependent negative feedback helps terminating puffs, and therefore the puff probability immediately after a puff is smaller than the stationary value but typically not 0. Channel clusters recover within a few seconds to the stationary puff probability[9,15,18,22–24].

The negative feedback terminating release spikes causes an *absolute* refractory period T_{min} as part of the interspike intervals (ISIs) lasting tens of seconds[25–27]. The molecular mechanism of this feedback is pathway and cell type specific and not always known although a negative feedback on the IP_3 concentration might be involved[28,29]. Hence, the negative feedback that determines the time scale of interspike intervals is different from the feedback contributing to interpuff intervals and requires global (whole cell) release events.

At very strong stimulation, cells exhibit a raised Ca^{2+} concentration of much longer duration than spikes which may oscillate[30,31], burst[32,33] or is rather constant[1,34,35]. Typically, the amplitude of these oscillations is smaller than the spike amplitude. In the following we review our current understanding of experimental results on Ca^{2+} signaling and how it illustrates the relation between mathematical structures and observations in biophysics.
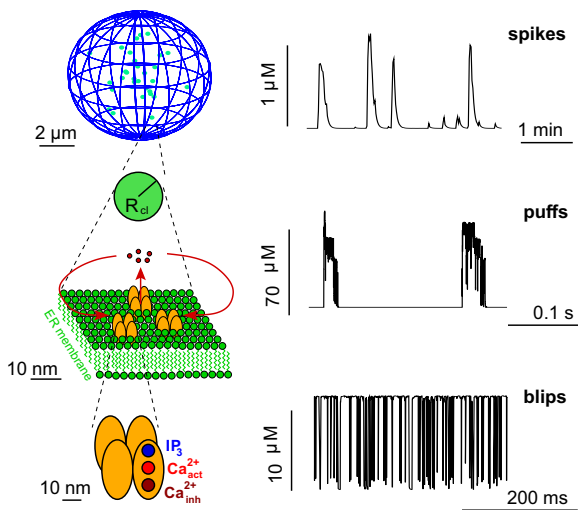
FIG. 1. Hierarchical organization of IP_3 induced Ca^{2+} signalling with concentration signals of the corresponding structural level. The elementary building block is the IP_3R channel (bottom). It opens and closes stochastically. An open channel entails Ca^{2+} release into the cytosol due to the large concentration difference between the ER and the cytosol. Since channels are clustered, opening of a single channel, which is called a blip, leads to activation of other channels in the cluster, i.e., a puff (middle). The cluster corresponds to a region with Ca^{2+} release with a radius R_{cl} that is fixed by the number of open channels. The stochastic local events are orchestrated by diffusion and CICR into cell wide Ca^{2+} waves, which form the spikes on cell level (top). (Figure reprinted from A. Skupin, H. Kettenmann, and M. Falcke, "Calcium signals driven by single channel noise" PLoS Comput Biol 6, e1000870 (2010).[36].)

II. EXPERIMENTAL RESULTS ON THE PHASE SPACE STRUCTURE AND DYNAMICAL PROPERTIES OF IP_3 INDUCED CA^{2+} RELEASE

The pathway exhibits local Ca^{2+} release through individual channel clusters at low $[IP_3]$, spiking at intermediate $[IP_3]$ and an elevated cytosolic $[Ca^{2+}]_i$ at high $[IP_3]$. A basic observation in all experiments is, that cell-to-cell variability with respect to Ca^{2+} spiking behavior is large but not completely arbitrary. It obeys some preserved characteristics, which have been confirmed for all cell types in which they have been investigated. We will focus on these general characteristics since they obviously reflect essential system properties.

It is convenient for the presentation of experimental results to introduce also a few mathematical concepts. In mathematical terms, intracellular Ca^{2+} dynamics are described by reaction-diffusion equations like

$$\frac{\partial X}{\partial t} = D \triangle X + F(X, \vec{r}, t, p), \qquad (1)$$

where X is a vector of concentrations, t is time, $\vec{r}$ is the space coordinate, D is a diagonal diffusion matrix, $\triangle$ the Laplace operator, $F(\cdot)$ is a non-linear function describ-

ing the local dynamics, and p is a vector of parameters. X comprises free cytosolic Ca^{2+}, Ca^{2+} bound to Ca^{2+}-binding molecules, IP_3, and free and bound Ca^{2+} in the lumen of the ER and mitochondria in a rather general formulation of the dynamics.

In general, non-linear dynamics reaches asymptotically the attractors in phase space which may be stationary states or manifolds of higher dimension. Attractors with higher dimension like limit cycles, tori or even chaotic attractors potentially describe the Ca^{2+} spiking behaviour. They may be caused by the dynamics of spatial modes (eigenfunctions of the linearized rhs of Eq. (1)) or by the local dynamics[37], i.e. may occur with $\triangle X \equiv 0$ also. Spatial modes have been observed with the Ca^{2+} dynamics of excitation contraction coupling in cardiac myocytes[38,39], which is a driven system in terms of dynamical systems theory. However, there is no experimental evidence for attractors of the autonomous and/or IP_3 induced intracellular Ca^{2+} dynamics caused by spatial modes, and hence we can focus on properties of the local dynamics.

The local dynamics of Eq. (1) are the behaviour of the IP_3R clusters. The majority of the modelling literature assumes oscillatory local dynamics in the spiking regime, since measured spikes are repetitive. Indeed, spike sequences even with a CV of 0.3-0.4 of the ISI appear surprisingly regular in visual inspection. However, a closer look could not confirm this assumption[24,40].

Clusters are dynamically coupled by Ca^{2+} diffusion, which needs to be reduced for investigations focussing on the local dynamics. Such an uncoupling can be achieved by high intracellular concentrations of the Ca^{2+} buffer EGTA. The elemental event of the local dynamics is the stochastic opening of channels in a cluster. The first open channel entails with some probability opening of more channels in the cluster causing a puff. Puffs last typically a few tens of ms but with large scatter[13,41]. The probability of triggering calcium puffs is linearly related to the number of IP_3R in a cluster[42]. Puff sequences at a given cluster exhibit some correlation between amplitude and subsequent interpuff intervals, a weak correlation between interpuff intervals and subsequent amplitude, but no detectable correlation between consecutive amplitudes[41]. Both puff amplitude and frequency increase and saturate with increasing stimulation of cells[42].

Typical interpuff intervals last a few seconds[13,24,41,42], interspike intervals are in the range from about 20 s to a few minutes. If the local dynamics were oscillatory and caused the sequence of spikes, the time scale of the ISI should be detectable as a temporal modulation of properties of the puff sequence at a given site. That has not been found[24]. A modulation of puff sequences on the ISI time scale could not be detected and no evidence of an oscillatory regime of the local dynamics has been observed[24]. The ISI time scale has only been observed on cell level. Consequently, spikes are a collective phenomenon requiring coupling of clusters. Another set of experiments demonstrated that indeed the average ISI depends sensitively on the intracellular buffer concentra-

tion modulating the strength of spatial coupling[40]. This confirms the results of the analysis of the local dynamics.

These experimental results are supported by theoretical investigations. The Ca^{2+} concentration at closed clusters is the resting concentration in the range of ≤ 100 nM. Detailed simulations of the concentration dynamics in the immediate vicinity of channels[14] showed that concentrations at open channels are high (>20 μM). The dynamic range of the regulatory binding sites for both the positive and negative feedback of Ca^{2+} to the open probability ranges from a few hundred nM to micromolar values below 10 μM [43–45]. Oscillatory dynamics require concentration values in the dynamic range. However, with these large concentration changes, the system essentially never is in this dynamic range and the regime of the deterministic limit of the cluster dynamics is either excitable or bistable (except tiny parameter ranges)[17].

If channels are sufficiently sensitized for Ca^{2+} binding, puffs may cooperate to set off a global release spike spreading from the initiating site into the cell in a wave like manner. Waves occur if a critical number of releasing clusters is reached[16,46,47]. The randomness of puffs causes randomness of spike timing with a linear relation between the standard deviation σ of interspike intervals (ISI) and the average T_{av}

$$\sigma = \alpha \left(T_{av} - T_{min} \right) \qquad (2)$$

as shown in Fig. 2 and further for 8 cell types and 10 conditions[27,40,48–50] (see also[51]). The slope α of this relation between SD and average is the same for all cells of the same type stimulated with the same agonist[27,40,48,49,52] and robust against changes in stimulation strength[27], pharmacological perturbations[27], changes in buffering conditions[40], and the large cell variability. It has been verified even in cells not exhibiting clustering of channels and puffs[49]. Values of α are for example about 0.2 for hepatocytes stimulated with vasopressin, 0.25 for HEK cells stimulated with CCh, 0.37 for hepatocytes stimulated with phenylephrine[27], 0.7 for PLA cells[52] and close to 1 for spontaneously spiking astrocytes[40]. Consequently, the standard deviation is of the same order of magnitude as the average ISI.

The standard deviation of ISI of oscillatory systems moving on a limit cycle in phase space and perturbed by noise is typically smaller than the values measured for Ca^{2+} spiking[53], and/or the cumulant relation may exhibit a negative slope[53]. Varying parameter values across the range covered by cell variability and the perturbations applied in two studies[27,40] causes loss of a unique relation between σ and T_{av}[53] with these oscillatory systems, since the period and the noise causing the standard deviation are determined by differential processes. Thus the robustness of α against cell variability and perturbations can hardly be reconciled with an oscillatory dynamics, since all these parameter variations against which α is robust would need to affect the processes setting the average and the processes setting the SD in exactly the way conserving the CV. But since spike generation is
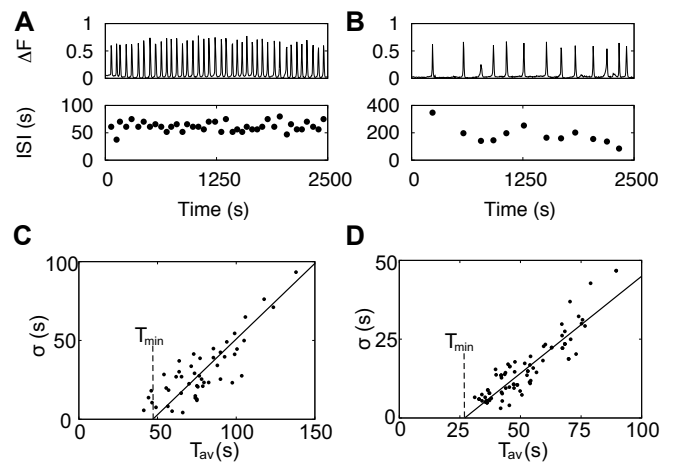

FIG. 2. Variability in Ca^{2+} signals. **A**: The transient cytosolic Ca^{2+} concentration of an astrocyte stimulated with 10 μM ATP (upper panel) exhibits some variability as indicated by the variable individual ISIs (lower panel). **B**: An astrocyte of the same experiments shows slower and more irregular spiking illustrating cell-to-cell variability. **C**: The systematic analysis of the standard deviation σ of ISI versus the average ISI T_{av} for HeLa cells stimulated with 100 μM histamine reveals a linear dependence in accordance with the moment relation (2) where each data point corresponds to the characteristic of an individual cell. **D**: The σ-T_{av} relation of astrocytes stimulated with 10 μM ATP exhibits also a linear dependence with a different slope than HeLa cells. T_{av}-T_{min} is the average stochastic part of the ISI.

stochastic, the parameters control only the spike generation probability, and the type of stochastic process – like e.g. inhomogeneous Poisson – fixes the relation between T_{av} and σ[54].

The second parameter of Eq. (2), the absolute refractory period T_{min}, was also found to be the same for all individual cells of the same type stimulated with the same agonist[27,40]. When T_{min} has passed, the puff probability recovers from 0 gradually to its asymptotic value. This slow recovery delays initiation of the next spike. That spike may occur during recovery, if the asymptotic spike generation probability is large compared to the recovery rate, or after recovery in the opposite case. The contribution of this stochastic part of the ISI to the total average ISI has been thoroughly investigated and is well known. It contributes typically 40%-70% to the total average ISI, and the measured range is from 8% to 95% contribution[27,40,48–50]. The recovery reduces also the SD (of the stochastic part) of the ISI[27,40,48–50]. The slower the recovery the smaller is the ratio of SD to average ISI (coefficient of variation CV)[54].

The wave-nucleation like generation of global release spikes as well as the ISI statistics strongly suggest excitability as the dynamic regime of IP_3 induced Ca^{2+} spiking in agreement with the analysis of the local dynamics. Excitable systems exhibit a stationary state
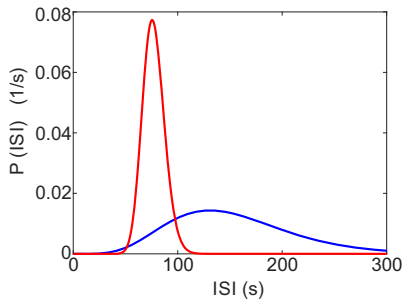
FIG. 3. ISI distributions P(ISI) for two spike trains measured with HEK cells stimulated with 100 μM CCh. The differences between the distributions illustrate cell variability. The experimental data are from the experiments published in ref.[27], the fitting method is explained in ref.[56].

which is stable against small perturbations. Perturbations above the excitation threshold are amplified to a transition to the excited state. The stochastic behavior of channel clusters causes incidental local transitions to the excited state, which then spreads with some probability into the whole cell. The resulting large fraction of open clusters - i.e. a release spike - causing a high Ca^{2+} concentration and high open probability are the excited state of Ca^{2+} dynamics. This state is terminated by negative feedback acting on a slower time scale than the excitation. The probability for generating this supercritical local excitation fixes the average stochastic part T_{av}-T_{min} and the standard deviation σ.

The complete distribution of ISI cannot be easily determined from experimental data since measured spike trains are not longer than about 60 ISI. Fusion of ISI sequences normalised by T_{av} have been used as a surrogate data set and led to skewed distributions with an absolute refractory period[55]. More sophisticated methods based on the time rescaling theorem and Kolmogorov-Smirnov tests for comparison of measured and hypothetical distributions identified an inhomogeneous Gamma distribution as the most likely experimental ISI distribution with time dependent stimulus[56]. Distributions of ISI obtained with these methods and constant stimulation are shown in Fig. 3.

The response of the average ISI to stimulation with extracellular agonists has features applying to all of the four plasma membrane receptors for which it has been investigated[27]. On that basis, we assume them also to be general features of the system. T_{min} is not affected by stimulation, as we have learned from the robustness properties of Eq. (2), already. Stimulation controls the average stochastic part T_{av}-T_{min} of the ISI. The concentration response has been established by applying steps in the concentration a of the stimulating agonist[27]. The change of the average stochastic part of the ISI due to this concentration step is proportional to the average stochastic part at the lower agonist concentration T_{av1}[27]:

$$\Delta T_{av} = \beta \left(T_{av1} - T_{min} \right). \qquad (3)$$

Analysis of measurements revealed that β does not depend on the agonist concentration[27], which entails an exponential dependency on a

$$T_{av} = T_{st}^{ref} e^{-\gamma(a-a^{ref})} + T_{min}. \qquad (4)$$

T_{st}^{ref} is the average stochastic part measured at the reference concentration a^{ref}. This prefactor of the exponential is cell specific and picks up all the cell variability. The constant γ in the exponent is the same for all cells of a given cell type stimulated with the same agonist. Eq. (4) does not bear directly information on the dynamic regime of IP_3 induced Ca^{2+} spiking, but it defines clear constraints to its theory.

III. BASIC REQUIREMENTS AND CONCEPTS FOR MODELLING OF IP₃ INDUCED INTRACELLULAR CA²⁺ DYNAMICS

A comprehensive monograph reviewing modelling of intracellular Ca^{2+} dynamics has recently been published[57]. Here, we would like to fill a void in the literature by a critical reflection on the framework of model derivation and the approximations coming with modelling concepts used in the biophysical literature.

The essence of the system is defined by its general properties, which are also the basic requirements models should meet:

- The sequence of dynamic regimes with increasing stimulation: puffs, spikes, permanently elevated Ca^{2+}. Pathway dependent also a bursting regime may follow or replace the spiking regime.

- The dynamics of individual clusters are not oscillatory on the time scale of ISI.

- Cell-to-cell variability of average ISI is large.

- The spiking regime obeys Eqs. (2), (3) and (4) with T_{min}, α and γ being cell type and pathway specific but not subjected to cell variability.[58]

- ISIs depend sensitively on parameters of spatial coupling.

The high stimulation regime is not in this list, since the behavior is cell type dependent - it might be stationary or oscillatory.

The hierarchical organization of CICR carries the randomness of individual channels onto the level of cell-wide spikes via the stochastic puff dynamics of clusters (Fig. 1). The random channel state changes are the source of noise. Consequently, the master equation for the probability of the microscopic states of the system is the starting point for an exact theory. In the most general case, that would comprise the position and number of Ca^{2+} ions and Ca^{2+} binding molecules and the state of the channels and pumps. While the master equation as the starting point for a theory defines concepts and

methods to be used, solving it is not practical in the end. Hence, probabilistic theories usually start from formulations of the state dynamics eligible for simulating trajectories in phase space.

A. Simulations

The diffusion coefficients of Ca^{2+} and Ca^{2+} binding molecules are sufficiently large to establish the deterministic concentration profile on the time scale of typical channel state changes due to the frequent sampling of space by thermal motion. The number of SERCA molecules is orders of magnitude larger than the number of Ca^{2+} channels. Hence, we can describe diffusion, the reactions involving cytosolic Ca^{2+} binding molecules and the SERCA flux by reaction-diffusion equations like Eq. (1). The opening and closing of channels causes time dependent source terms in the partial differential equation for the Ca^{2+} concentration. We illustrate that with a simple model comprising cytosolic Ca^{2+} c, one Ca^{2+} buffer b (Ca^{2+} bound form) and the ER Ca^{2+} concentration e

$$\frac{\partial c}{\partial t} = D_c \triangle c + \sum_{i=1}^{N} \sum_{j=1}^{\infty} A_{i,j}(c,e)\, \delta(t-t_{i,j})\, \delta(\vec{r}-\vec{r_i})$$
$$-V_p \frac{c^2}{K^2+c^2} + P_l(e-c) - k^+(b_t-b)c + k^-b \quad (5)$$

$$\frac{\partial e}{\partial t} = D_e \triangle e - \nu \left[\sum_{i=1}^{N_p} \sum_{j=1}^{\infty} A_{i,j}(c,e)\, \delta(t-t_{i,j})\, \delta(\vec{r}-\vec{r_i}) \right.$$
$$\left. +V_p \frac{c^2}{K^2+c^2} - P_l(e-c) \right] \quad (6)$$

$$\frac{\partial b}{\partial t} = D_b \triangle b + k^+(b_t-b)c - k^-b. \quad (7)$$

Here, b_t denotes the total buffer concentration, k^+ and k^- the binding and dissociation rate, V_p is the maximum SERCA pump flux, and ν the ratio of cytosol to ER volume. We have approximated the shape of a channel mouth by a spatial δ-function and the time course of a single opening by a temporal δ-function. N is the number of channels, $\vec{r_i}$ is the location of the ith channel, and $\{t_{i,j}\}$ the sequence of its openings before time t. The sequence of time points of openings is determined by Markov chain Monte Carlo simulations for the state of each individual channel. The simulations are based on state schemes, an example is shown in Fig. 4. Such an approach has been used both for single clusters as well as cell-wide cluster arrays[19,53,59–64].

This type of simulations is well suited to investigate channel state schemes in cellular context, the role of particular pathway components or spatial aspects[19,53,59,62–64].

B. Distributions and their moments

Probability distributions for stochastic variables are the natural way to characterize stochastic systems. They are the solutions of the master equation. However, we need to simplify the system to obtain equations we can solve. These simplified systems can be informed by the general properties listed above. We know about the ISI distribution that it should exhibit an absolute refractory period and a linear relation between standard deviation and average.

The formulation of the problem in terms of Eq. (5) and Markov chains can also serve as starting point for analytical calculations or derivation of simplified models. The robustness of spike generation with respect to cell variability and perturbations demonstrates that it cannot depend on very specific parameter values or other details. Hence, simplifications should not destroy the basic characteristics of the system. At the same time, the large cell variability entails requirements on the theory. With each experiment comprising a population of cells we sample a phase space volume large enough for accommodating this cell variability. Hence, the qualitative properties of IP_3 induced Ca^{2+} dynamics listed above must not depend sensitively on the value of parameters distinguishing individual cells. These parameters comprise protein concentrations[65], the number of clusters, their spatial arrangement, diffusion properties and more[13].

A suggestion for calculating the ISI distribution has been made in this spirit[54]. It starts from the wave nucleation character of spike generation. All clusters are closed at the end of a spike. Each opening cluster entails a sphere of increased Ca^{2+} concentration around it. We indicate that by the orange spheres in the red round cells above scheme (8). The local rise in Ca^{2+} increases the open probability of the open cluster's neighbours. A spike occurs, when a critical number N_{cr} of open clusters is reached via one of many possible paths of cluster openings. Hence, the ISI calculation can be formulated as a first passage problem from 0 to N_{cr} open clusters. The first passage time distribution corresponds to the ISI distribution for stationary spike trains. This approach radically simplifies the system into a state space defined by the number of open clusters only[54]. That implies averaging over all N_{path} possible paths from 0 to N_{cr} open

cluster[54]:

$$(8)$$
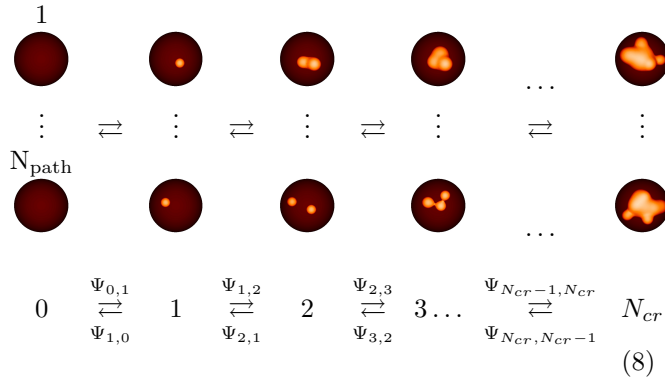
The transition probabilities from k to $k+1$ open clusters are determined by the probability that k open clusters open another one, and from k to k-1 that a cluster closes. The transition probabilities $\Psi_{i,k}$ in state scheme (8) can be directly calculated from interpuff interval and puff duration distributions[54]. Such an approach is able to explain the cumulant relation Eq. (2)[54].

A lot remains to be done even with such a simple approach. The dependency of the transition probability on the numbers of open clusters and the parameters of spatial coupling has not been worked out analytically, yet. Also, the effect of the recovery from the negative feedback terminating spikes has not yet been described analytically in this approach but with phenomenological ansatzes or stochastic simulations only[40,53,55,66]. A new approach to this problem has been suggested recently, but has not been specified to Ca^{2+} spiking, yet[67]. Derivation of the concentration response relation Eq. (4) with this approach has neither been attempted, yet.

C. Rate equations

Rate equations for lumped variables might be desirable for simplified models and have been successfully used for investigating specific aspects of pathways or the dynamics[3,28,57,70–74]. The derivation of rate equations implies averaging over the state distribution dynamics defined by the master equation. The spatial character of spike initiation renders the averaging difficult. Another (related) conceptual problem arises from the fact that the dynamics on cell level is still noisy. In contrast, the more frequent situation in the derivation of cellular dynamics encounters noise on the molecular level only. The population average carried out in the master equation of such systems during the derivation of rate equations is an average over the molecules in a single cell. The large number limit guaranteeing the validity of deterministic rate equations applies to the cell level. With IP_3 induced Ca^{2+} spiking, this limit does not apply to the cell level, since cell behavior is noisy. The average needs to be carried out across an ensemble of identical cells.

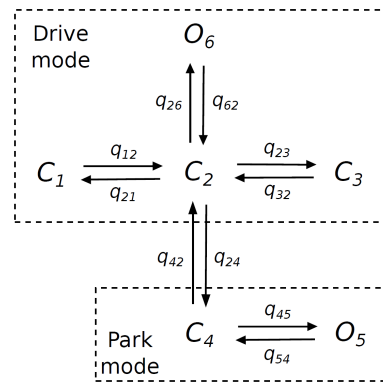Consequences of these considerations can be illustrated by a comparison to existing rate equation models. We

FIG. 4. This state scheme of the IP_3R originally published by Siekmann et al.[68] is comprised of two modes. One is the drive mode containing three closed states C_1, C_2, C_3 and one open state O_6. The other is the park mode which includes one closed state C_4 and one open state O_5. The rates of state-transitions within each mode are constants. α and β are the rates connecting the two modes and depend on Ca^{2+} in a highly dynamic manner. Figure reprinted with permission from Biophysical Journal 112(2017) , P. Cao, M. Falcke, and J. Sneyd, "Mapping interpuff interval distribution to the properties of inositol trisphosphate receptors", 2138–2146, copyright (2018)[69].

prepare this comparison by reconsidering the rate equation derivation of the most simple stochastic process - radioactive decay of atoms. The stochastic variable is the number N_a of atoms. We denote the probability per unit time for decay of a single atom with λ. The atom number N_a obeys for large initial numbers N_i the exponential function $N_a = N_i e^{-\lambda t}$. Each decaying atom is in a stationary state till it decays, there is no process setting the time point of its decay. However, if we ask for the time t_r required till a specific number of atoms N_r remains in the deterministic limit, it is set by N_i, N_r and λ ($t_r = \lambda^{-1} \ln(N_i/N_r)$). The process setting the time scale is the continuous decrease of N_a down to N_r.

Rate equation models derived by averaging on the molecular level and assuming deterministic behavior on cell level usually require specific processes to set the time scale of ISIs. That might be a rising fraction of channels recovered from inhibition, an approach to a critical Ca^{2+} concentration or the rise of receptor sensitization[57,74]. However, the noisy behavior of Ca^{2+} spiking entails different determinants of the average ISI. Figure 5 illustrates some differences between the rate equations obtained by assuming deterministic cell behavior and noisy behavior on cell level. The time courses were obtained from simulations of a purely deterministic model[75] (black) and a noisy excitable version of it[53] (red). Both systems respond with a spike to the perturbation. The noisy system generates subsequent spikes some time after the stimulated one (red line in Fig. 5A). The deterministic rate equation model stays in a stationary state after the initial perturbation without generating a second spike (black line in Fig. 5A). During the time T_{div}, the
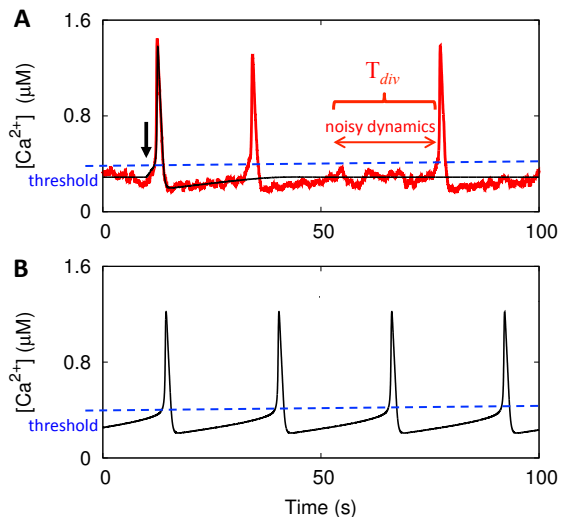
FIG. 5. Time scales set by noise are not captured by current deterministic rate equations. **A**: Caricature of a Ca^{2+} time course as produced by deterministic rate equations (black) and by a corresponding noisy system (red) after an initial perturbation (arrow) based on model simulations[53,75]. The noisy system generates subsequent spikes some time after the previous one. During the time T_{div}, the deterministic rate equations are in a stationary state without generating a second spike. **B**: The interspike interval is dominated by the time required to reach the threshold of CICR (blue) in the oscillatory regime of deterministic rate equation models. The dependency of the ISI on the parameters characterizing the noise is lost.

dynamics is completely noise dominated. This illustrates that completely analogous to radioactive decay, there is no deterministic process on the level of the individual cell setting its ISI after recovery from the previous spike.

Spiking is lost in the rate equations since T_{div} diverges due to averaging on the molecular level. Thus also the dependency of the ISI on the parameters characterizing the noise and spatial coupling is lost. Most rate equation models tune parameters to an oscillatory regime to establish spiking (Fig. 5B). The interspike interval is then dominated by the time required to reach the threshold for CICR. This entails parameter dependencies of the ISI different from the ones of noise driven dynamics.

The sketch of T_{div} for the excitable model in Fig. 5A applies when the asymptotic spike generation probability reached after recovery is smaller than the recovery rate from negative feedback. The medium and long ISI data in Xenopus oocytes[18] and spontaneously spiking astrocytes and microglia cells[40,66] are experimental realizations. Their recovery phase from negative feedback is substantially shorter ($\alpha \approx 1$) than the average ISI[40,66]. The effect of noise on time scales and parameter dependencies is also substantial if the recovery phase and the average ISI are of comparable length[27,40,66].

In summary, averaging on the single cell level across molecules and clusters eliminates the noise generating the

spike. The rate equations for this average do not reflect the spike generating mechanism, since usually an oscillatory regime is then used to 'rescue' spiking. However, averaging over a stochastic ensemble of cells defined by a cellular spike generation probability distribution allows for including the average of the noise generated time scale and its parameter dependencies, and can thus reflect the spike generation mechanism.

Deriving rate equations in a way reflecting the spike generation mechanism is an open problem and has not been attempted, yet. Suitable concepts might be inspired by the integrate-and-fire models of neuronal dynamics starting from an expression for the spike generation probability on cell level. Investigations on globally coupled noisy excitable systems might be specified to Ca^{2+} dynamics[76]. Another very promising approach includes higher moments in the derivation[77].

Parameter dependencies and the mathematical structure of models can also be restricted by Eqs. (3) and (4). Stochastic simulations of the excitable regime of the frequently used DeYoung-Keizer-model reproduced Eq. (3) but not Eq. (4). Hence, a comprehensive theoretical understanding of the concentration response is still lacking.

IV. CONCLUSION

While detailed multiscale simulations can mimic experimental observations in a rather flexible manner[19,53,59–64], neither the current state of the stochastic theory, nor the rate equation models live up to the request for predicting experimental outcome beyond the examples used for model derivation. This indicates that we have not yet understood how to derive the appropriate models. Based on the accordance of experimental and multiscale simulation results, we come to the conclusion that a reaction diffusion system with a local dynamics in a noisy excitable regime must be the starting point of the derivation of predictive models, since it is the mathematical structure corresponding to the observations.

IP_3 induced Ca^{2+} dynamics is a classic of biological applications of non-linear dynamics[57,78–80]. On the basis of early interpretations of experimental results, it became one of the prototypical cellular limit cycle oscillators. The recent experimental results reviewed in this study revealed that the repetition of spikes is caused by noise instead of a limit cycle or torus in phase space. Derivation of predictive and simple models starting from this noisy spatially extended excitable system is a task reaching beyond the specific biological system. Hence, this classic still poses theoretical problems interesting and challenging for the whole field of nonlinear dynamics.

of Health.

[1] L. Jouaville, F. Ichas, E. Holmuhamedov, P. Camacho, and J. Lechleiter, "Synchronisation of calcium waves of mitochondrial substrates in Xenopus laevis oocytes," Nature **377**, 438–441 (1995).

[2] M. Falcke, M. Bär, J. Lechleiter, and J. Hudson, "Spiral breakup and defect dynamics in a model for intracellular Ca^{2+} dynamics," Physica D **129**, 236–252 (1999).

[3] M. Falcke, "Reading the patterns in living cells - the Physics of Ca^{2+} signaling," Advances in Physics **53**, 255–440 (2004).

[4] M. Falcke, J. Hudson, P. Camacho, and J. Lechleiter, "Impact of mitochondrial Ca^{2+} cycling on pattern formation and stability," Biophys.J. **77**, 37–44 (1999).

[5] M. Falcke, Y. Li, J. Lechleiter, and P. Camacho, "Modeling the dependence of the period of intracellular Ca^{2+} waves on SERCA expression," Biophys.J. **85**, 1474–1481 (2003).

[6] M. Berridge, M. Bootman, and P. Lipp, "Calcium - a life and death signal," Nature **395**, 645–648 (1998).

[7] C. Taylor, "Why do hormones stimulate Ca^{2+} mobilization," Biochem.Soc.Trans. **23**, 637–642 (1995).

[8] G. Dupont, L. Combettes, G. S. Bird, and J. W. Putney, "Calcium oscillations," Cold Spring Harbor Perspectives in Biology **3** (2011).

[9] M. Bootman, E. Niggli, M. Berridge, and P. Lipp, "Imaging the hierarchical Ca^{2+} signalling in HeLa cells," J.Physiol **499**, 307–314 (1997).

[10] I. F. Smith, S. M. Wiltgen, and I. Parker, "Localization of puff sites adjacent to the plasma membrane: Functional and spatial characterization of Ca^{2+} signaling in SH-SY5Y cells utilizing membrane-permeant caged IP_3," Cell Calcium **45**, 65–76 (2009).

[11] Taufiq-Ur-Rahman, A. Skupin, M. Falcke, and C. W. Taylor, "Clustering of $InsP_3$ receptors by $InsP_3$ retunes their regulation by $InsP_3$ and Ca^{2+}," Nature **458**, 655–659 (2009).

[12] W. Suhara, M. Kobayashi, H. Sagara, K. Hamadad, T. Goto, I. Fujimoto, K. Torimitsu, and K. Mikoshiba, "Visualization of inositol 1,4,5-trisphosphate receptor by atomic force microscopy," Neuroscience Letters **391**, 102–107 (2006).

[13] M. V. Keebler and C. W. Taylor, "Endogenous signalling pathways and caged ip3 evoke ca2+ puffs at the same abundant immobile intracellular sites," Journal of Cell Science **130**, 3728–3739 (2017).

[14] R. Thul and M. Falcke, "Release currents of IP_3 receptor channel clusters and concentration profiles," Biophys.J. **86**, 2660–2673 (2004).

[15] Y. Yao, J. Choi, and I. Parker, "Quantal puffs of intracellular Ca^{2+} evoked by inositol trisphosphate in Xenopus oocytes," J Physiol **482**, 533–553 (1995).

[16] J. Marchant, N. Callamaras, and I. Parker, "Initiation of IP3-mediated Ca^{2+} waves in Xenopus oocytes," The EMBO J. **18**, 5285–5299 (1999).

[17] R. Thul and M. Falcke, "Stability of membrane bound reactions," Phys Rev Lett **93**, 188103 (2004).

[18] J. Marchant and I. Parker, "Role of elementary Ca^{2+} puffs in generating repetitive Ca^{2+} oscillations," The EMBO Journal **20**, 65–76 (2001).

[19] M. Falcke, "On the role of stochastic channel behavior in intracellular Ca^{2+} dynamics," Biophys.J. **84**, 42–56 (2003).

[20] H. Schulman, P. Hanson, and T. Meyer, "Decoding calcium signals by multifunctional cam kinase," Cell Calcium **13**, 401 – 411 (1992).

[21] W. Li, J. Llopis, M. Whitney, M. Zlokarnik, and R. Tsien, "Cell-permeant caged $InsP_3$ ester shows that Ca^{2+} spike frequency can optimize gene expression," Nature **392**, 936–941 (1998).

[22] I. Parker, J. Choi, and Y. Yao, "Elementary events of $InsP_3$-induced Ca^{2+} liberation in Xenopus oocytes: hot spots, puffs and blips," Cell Calcium **20**, 105–121 (1996).

[23] E. R. Higgins, H. Schmidle, and M. Falcke, "Waiting time distributions for clusters of IP_3 receptors," Journal of Theoretical Biology **259**, 338 – 349 (2009).

[24] K. Thurley, I. F. Smith, S. C. Tovey, C. W. Taylor, I. Parker, and M. Falcke, "Timescales of IP3-evoked Ca^{2+} spikes emerge from Ca^{2+} puffs only at the cellular level," Biophys J **101**, 2638–2644 (2011).

[25] N. Woods, K. Cuthbertson, and P. Cobbold, "Repetitive transient rises in cytoplasmic free calcium in hormone-stimulated hepatocytes," Nature **319**, 600–602 (1986).

[26] T. Rooney, E. Sass, and A. Thomas, "Characterization of cytosolic calcium oscillations induced by phenylephrine and vasopressin in single fura-2-loaded hepatocytes," J.Biol.Chem. **264**, 17131–17141 (1989).

[27] K. Thurley, S. C. Tovey, G. Moenke, V. L. Prince, A. Meena, A. P. Thomas, A. Skupin, C. W. Taylor, and M. Falcke, "Reliable encoding of stimulus intensities within random sequences of intracellular Ca^{2+} spikes," Sci. Signal. **7**, ra59 (2014).

[28] A. Politi, L. D. Gaspers, A. P. Thomas, and T. Höfer, "Models of IP_3 and Ca^{2+} oscillations: Frequency encoding and identification of underlying feedbacks," Biophys J **90**, 3120 – 3133 (2006).

[29] P. J. Bartlett, W. Metzger, L. D. Gaspers, and A. P. Thomas, "Differential regulation of multiple steps in inositol 1,4,5- trisphosphate signaling by protein kinase C shapes hormone-stimulated Ca^{2+} oscillations." Journal of Biological Chemistry (2015).

[30] M. Berridge, "Calcium oscillations," J.Biol.Chem. **265**, 9583–9586 (1990).

[31] M. Nash, K. Young, R. Challiss, and S. Nahorski, "Receptor-specific messenger oscillations," Nature **413**, 381–382 (2001).

[32] A. Green, P. Cobbold, and C. Dixon, "Elevated intracellular cyclic AMP exerts different modulatory effects on cytosolic free Ca^{2+} oscillations in single rat hepatocytes," Biochem.J. **302**, 949–955 (1994).

[33] A. Green, C. Dixon, A. McLennan, P. Cobbold, and M. Fisher, "Adenine dinucleotide-mediated cytosolic free Ca^{2+} oscillations in single hepatocytes," FEBS **322**, 197–200 (1993).

[34] M. S. Nash, M. J. Schell, P. J. Atkinson, N. R. Johnston, S. R. Nahorski, and R. A. J. Challiss, "Determinants of Metabotropic Glutamate Receptor-5-mediated Ca^{2+} and Inositol 1,4,5-Trisphosphate Oscillation Frequency," J Biol Chem **277**, 35947–35960 (2002).

[35] M. Bootman, C. Taylor, and M. Berridge, "The thiol reagent, thimerosal, evokes Ca^{2+} spikes in HeLa cells by sensitizing the inositol 1,4,5-trisphosphate receptor," J.Biol.Chem. **267**, 25113–25119 (1992).

[36] A. Skupin, H. Kettenmann, and M. Falcke, "Calcium signals driven by single channel noise," PLoS Comput Biol **6**, e1000870 (2010).

[37] A. Mikhailov, *Foundations of Synergetics*, Springer Series in Synergetics, Vol. 1,2 (Springer, 1994).

[38] M. Diaz, D. Eisner, and S. O'Neill, "Depressed Ryanodine Receptor Activity Increases Variability and Duration of the Systolic Ca^{2+} Transient in Rat Ventricular Myocytes," Circ Res **91**, 585–593 (2002), http://circres.ahajournals.org/cgi/reprint/91/7/585.pdf.

[39] J. Kockskämper and L. A. Blatter, "Subcellular Ca^{2+} alternans represents a novel mechanism for the generation of arrhythmogenic Ca^{2+}+ waves in cat atrial myocytes," J Physiol **545**, 65–79 (2002), http://jp.physoc.org/cgi/reprint/545/1/65.pdf.

[40] A. Skupin, H. Kettenmann, U. Winkler, M. Wartenberg, H. Sauer, S. C. Tovey, C. W. Taylor, and M. Falcke, "How does intracellular Ca^{2+} oscillate: by chance or by the clock?" Biophys J **94**, 2404–11 (2008).

[41] G. D. Dickinson and I. Parker, "Factors determining the recruitment of inositol trisphosphate receptor channels during calcium puffs," Biophys J **105**, 2474 – 2484 (2013).

[42] G. D. Dickinson, D. Swaminathan, and I. Parker, "The probability of triggering calcium puffs is linearly related to the number of inositol trisphosphate receptors in a cluster," Biophys J **102**, 1826 – 1836 (2012).

[43] C. Taylor, "Inositol trisphosphate receptors: Ca^{2+}-modulated intracellular Ca^{2+} channels," Biochimica and Biophysica Acta **1436**, 19–33 (1998).

[44] J. K. Foskett, C. White, K.-H. Cheung, and D.-O. D. Mak, "Inositol trisphosphate receptor Ca^{2+} release channels," Physiological Reviews **87**, 593–658 (2007).

[45] E. Gin, M. Falcke, L. E. Wagner, D. I. Yule, and J. Sneyd, "A kinetic model of the inositol trisphosphate receptor based on single-channel data," Biophys.J. **96**, 4053–4062 (2009).

[46] G. Dupont, S. Swillens, C. Clair, T. Tordjmann, and L. Combettes, "Hierarchical organisation of calcium signals in hepatocytes: from experiments to models," Biochim.Biophys.Acta **1498**, 134–152 (2000).

[47] W. Croft, K. Reusch, A. Tilunaite, N. A. Russell, R. Thul, and T. C. Bellamy, "Probabilistic encoding of stimulus strength in astrocyte global calcium signals," Glia **64**, 537–552 (2016).

[48] S. Dragoni, U. Laforenza, E. Bonetti, F. Lodola, C. Bottino, R. Berra-Romani, G. Carlo Bongio, M. P. Cinelli, G. Guerra, P. Pedrazzoli, V. Rosti, F. Tanzi, and F. Moccia, "Vascular endothelial growth factor stimulates endothelial colony forming cells proliferation and tubulogenesis by inducing oscillations in intracellular Ca^{2+} concentration," Stem Cells **29**, 1898–1907 (2011).

[49] P. Cao, X. Tan, G. Donovan, M. J. Sanderson, and J. Sneyd, "A deterministic model predicts the properties of stochastic calcium oscillations in airway smooth muscle cells," PLoS Comput Biol **10**, e1003783 (2014).

[50] G. Dupont, A. Abou-Lovergne, and L. Combettes, "Stochastic Aspects of Oscillatory Ca^{2+} Dynamics in Hepatocytes," Biophys J **95**, 2193–2202 (2008).

[51] M. Perc, A. K. Green, C. J. Dixon, and M. Marhl, "Establishing the stochastic nature of intracellular calcium oscillations from experimental data," Biophys Chem **132**, 33 – 38 (2008).

[52] A. Skupin and M. Falcke, "The role of IP$_3$R clustering in Ca^{2+} signaling," Genome Informatics **20**, 15–24 (2008), skupin, Alexander Falcke, Martin Japan Genome informatics. International Conference on Genome Informatics Genome Inform. 2008;20:15-24.

[53] A. Skupin and M. Falcke, "From puffs to global Ca^{2+} signals: How molecular properties shape global signals," Chaos **19**, 037111 (2009).

[54] K. Thurley and M. Falcke, "Derivation of Ca^{2+} signals from puff properties reveals that pathway function is robust against cell variability but sensitive for control," Proc Nat Acad Sci USA **108**, 427–432 (2011).

[55] Skupin, A. and Falcke, M., "Statistical analysis of calcium oscillations," Eur. Phys. J. Special Topics **187**, 231–240 (2010).

[56] A. Tilūnaitè, W. Croft, N. Russell, T. C. Bellamy, and R. Thul, "A bayesian approach to modelling heterogeneous calcium responses in cell populations," PLOS Computational Biology **13**, 1–25 (2017).

[57] G. Dupont, M. Falcke, V. Kirk, and J. Sneyd, *Models of Calcium Signalling*, edited by S. Antman, L. Greengard, and P. Holmes, Interdisciplinary Applied Mathematics, Vol. 43 (Springer, 2016).

[58] We expect the ISI properties also to apply to interburst intervals with the slight modification of measuring the interburst interval from the end of a burst to the onset of the subsequent one.

[59] J. Keizer and G. Smith, "Spark-to-wave transition: saltatory transmission of calcium waves in cardiac myocytes," Biophys.Chem. **72**, 87–100 (1998).

[60] J. Shuai and P. Jung, "Optimal ion channel clustering for intracellular calcium signaling," Proc.Nat.Acad.Sci.USA **100**, 506–510 (2003).

[61] G. Ullah and P. Jung, "Modeling the Statistics of Elementary Calcium Release Events," Biophys J **90**, 3485–3495 (2006).

[62] S. Rüdiger, C. Nagaiah, G. Warnecke, and J. Shuai, "Calcium domains around single and clustered ip$_3$ receptors and their modulation by buffers," Biophys J **99**, 3 – 12 (2010).

[63] S. Rüdiger, P. Jung, and J.-W. Shuai, "Termination of ca^{2+} release for clustered ip$_3$r channels," PLoS Comput Biol **8**, e1002485 (2012).

[64] J. Shuai, J. E. Pearson, and I. Parker, "Modeling Ca^{2+} Feedback on a Single Inositol 1,4,5-Trisphosphate Receptor and Its Modulation by Ca^{2+} Buffers," Biophys J **95**, 3738–3752 (2008).

[65] A. Sigal1, R. Milo, A. Cohen, N. Geva-Zatorsky, Y. Klein, Y. Liron, N. Rosenfeld, T. Danon, N. Perzov, and U. Alon1, "Variability and memory of protein levels in human cells," Nature **444**, 643–646 (2006).

[66] A. Skupin and M. Falcke, "Statistical Properties and Information Content of Calcium Oscillations," Genome Informatics **18**, 44–53 (2007).

[67] M. Falcke and V. N. Friedhoff, "The Stretch to Stray on Time: Resonant Length of Random Walks in a Transient," (2018), arXiv:1801.05446.

[68] I. Siekmann, L. E. W. II, D. Yule, E. J. Crampin, and J. Sneyd, "A kinetic model for type i and {II} {IP3R} accounting for mode changes," Biophys J **103**, 658 – 668 (2012).

[69] P. Cao, M. Falcke, and J. Sneyd, "Mapping interpuff interval distribution to the properties of inositol trisphosphate receptors," Biophysical Journal **112**, 2138 – 2146 (2017).

[70] U. Kummer, L. Olsen, C. Dixon, A. Green, E. Bornberg-Bauer, and G. Baier, "Switching from simple to complex oscillations in calcium signaling," Biophys.J. **79**, 1188–1195 (2000).

[71] T. Haberichter, M. Marhl, and R. Heinrich, "Birhythmicity, trirhythmicity and chaos in bursting calcium oscillations," Biophys.Chem. **90**, 17–30 (2001).

[72] U. Kummer, B. Krajnc, J. Pahle, A. K. Green, C. J. Dixon, and M. Marhl, "Transition from Stochastic to Deterministic Behavior in Calcium Oscillations," Biophys J **89**, 1603–1611 (2005).

[73] G. Dupont, G. Houart, and A. Goldbeter, "From simple to complex Ca^{2+} oscillations: Regulatory mechanisms and theoretical models," (Springer, Berlin Heidelberg New York, 2003) Chap. 8, pp. 129–151.

[74] J. Sneyd, J. M. Han, L. Wang, J. Chen, X. Yang, A. Tanimura, M. J. Sanderson, V. Kirk, and D. I. Yule, "On the dynamical structure of calcium oscillations," Proc Nat Acad Sci USA **114**, 1456–1461 (2017).

[75] A. Goldbeter, G. Dupont, and M. J. Berridge, "Minimal model for signal-induced Ca^{2+} oscillations and for their frequency encoding through protein phosphorylation," Proc Nat Acad Sci USA **87**, 1461–1465 (1990).

[76] T. Prager, M. Falcke, L. Schimansky-Geier, and M. A. Zaks, "Non-markovian approach to globally coupled excitable systems," Physical Review E **76**, 011118 (2007).

[77] M. A. Zaks, X. Sailer, L. Schimansky-Geier, and A. B. Neiman, "Noise induced complexity: From subthreshold oscillations to spiking in coupled excitable systems," Chaos: An Interdisciplinary Journal of Nonlinear Science **15**, 026117 (2005).

[78] J. Murray, *Mathematical Biology* (Springer-Verlag, Berlin Heidelberg, 1993).

[79] A. Goldbeter, *Biochemical Oscillations and Cellular Rhythms* (Cambridge University Press, Cambridge, 1996).

[80] J. Keener and J. Sneyd, *Mathematical Physiology* (Springer, New York, 1998).